# $CaBPO_5$:$Dy^{3+}$, $Na^+$: A potential single-phased white-light-emitting phosphor under near ultraviolet excitation

BING HAN*, JIE ZHANG, YAN LIU, QIAO CUI
*School of Material and Chemical Engineering, Zhengzhou University of Light Industry, Zhengzhou 450002, People's Republic of China*

A series of phosphors $Ca_{1-2x}Dy_xNa_xBPO_5$ were synthesized by using a high-temperature solid-state reaction technique, and their UV-vis luminescence properties were investigated. The f–f transitions of $Dy^{3+}$ in the host lattice were assigned and discussed. The influence of the doping concentration on the relative emission intensity was investigated, and the optimum doping concentration is 0.02. The concentration quenching mechanism of $Dy^{3+}$ emission was discussed, indicating that dipole–dipole interaction dominated in $Dy^{3+}$ emission.

(Received March 24, 2012; accepted June 6, 2012)

*Keywords*: Phosphor, luminescence, White-light emitting, $Dy^{3+}$

## 1. Introduction

White light-emitting diodes (LEDs) are considered as the next generation light source because of their high brightness, long lifetime and environment friendliness [1-3]. Currently, combining an ultraviolet (UV) chip with down-converted tricolor phosphors is an ordinary way to obtain white LEDs. This approach provides white LEDs with high color render index and good color uniformity, as the white light are generated only by phosphors [4, 5]. However, in the three-converter system, the green or red-emitting phosphors can re-absorb the blue emission from the blue-emitting phosphor, which results in low luminous efficiency. Therefore, it is highly required to pay attention to the research on the single-host white phosphor under UV excitation for UV LED chip [6-8].

In the past few years more and more attention has been paid to $Dy^{3+}$ luminescence due to its potential practical application [9-11]. It is well known that a $Dy^{3+}$ ion with a $4f^9$ electronic configuration generally has two dominant emission bands in visible range: the blue band (480 nm) corresponds to the $^4F_{9/2}\rightarrow{}^6H_{15/2}$ transition, the yellow band (575 nm) corresponds to the hypersensitive $^4F_{9/2}\rightarrow{}^6H_{13/2}$ ($\Delta L = 2$, $\Delta J = 2$) transition, respectively. Obviously, the emitting color and the chromaticity coordinates are mainly decided by $^4F_{9/2}\rightarrow{}^6H_J$ (J = 15/2, 13/2) transitions for $Dy^{3+}$ ions. At a suitable lattice site, white-light emitting can be fulfilled by these emission bands [12]. As the hypersensitive transition $^4F_{9/2}\rightarrow{}^6H_{13/2}$ is influenced strongly by the crystal-field environment, the yellow-to-blue emission intensity ratio also reflects the coordination surroundings of $Dy^{3+}$ to some extent. So the research on $Dy^{3+}$-doped materials becomes more and more significant not only for basic research but also for potential industrial applications.

$CaBPO_5$[13, 14] belongs to the stillwellite type compounds with the trigonal system, space group $P3_121$, $Ca^{2+}$ ions are 10-fold coordinated by $O^{2-}$ ions in the form of $C_2$ symmetry. The arrangements of $BO_4^{5-}$ and $PO_4^{3-}$ were loop-branched chains. The central three single chains of $BO_4$ tetrahedra run parallel to [0 0 1], the $BO_4$ units were linked to terminal $PO_4$ tetrahedra. Considering the excellent thermal and chemical stability of such kind of borophosphates, $CaBPO_5$ was chosen to be the host lattice in the $Dy^{3+}$ ion doped phosphors in this paper. The main objective of this work is to investigate the preparation and photoluminescence properties of $CaBPO_5$:$Dy^{3+}$ phosphor in detail. A white light was observed under UV excitation, suggesting that this phosphor might be a promising UV-convertible candidate for white LEDs.

## 2. Experimental

The phosphors $Ca_{(1-2x)}Dy_xNa_xBPO_5$ (x = 0, 0.005, 0.01, 0.02, 0.03, 0.04, 0.05) were synthesized by a high-temperature solid-state reaction technique. The starting materials are analytical reagent (A.R.) grade $CaCO_3$, $H_3BO_3$, $NH_4H_2PO_4$, and $Dy_2O_3$ (99.99 %). $Na_2CO_3$ was added as a charge compensator because the substitution of a $Dy^{3+}$ ion for an alkaline earth ion requires the presence of a charge compensator to maintain overall charge neutrality of the crystal. The stoichiometric reactants were mixed and ground thoroughly in an agate mortar. Then the mixture was pre-heated at 500 °C for 2 hours in a muffle furnace, reground and finally fired at 1000 °C for 4 hours in air atmosphere. After the reaction at 1000 °C, the products were cooled down slowly to room temperature (RT) by switching off the muffle furnace and ground into white power.

The phase purity and structure of the final products was characterized by a powder X-ray diffraction (XRD) analysis with Cu $K_\alpha$ ($\lambda$ = 1.5405 Å) radiation on a D8 Advance X-Ray Diffractometer at 40 kV and 20 mA. Photoluminescence (PL) and photoluminescence excitation (PLE) spectra were measured on a fluorescence spectrometer (HITACHI F-7000) equipped with a 450 W xenon lamp as the excitation source at room temperature. The excitation and emission slits were set at 1 nm, all the spectra were measured at a scan speed of 240 nm/min.

## 3. Results and discussion

The XRD pattern of a $CaBPO_5$ sample is displayed in Fig. 1(b). It agrees with the JCPDS standard card in Fig. 1(a), which indicates the formation of a pure single $CaBPO_5$ phase. The samples $Ca_{(1-2x)}Dy_xNa_xBPO_5$ with different doping concentration (x value) are also single phases that are in line with the undoped sample $CaBPO_5$ in Fig. 1(b) as well as the JCPDS 18-0283 [$CaBPO_5$] standard card in Fig. 1(a). As an example, the diffractogram of a $Dy^{3+}$-doped sample $CaBPO_5$ is exhibited in Fig. 1(c). The results show that a single phase was formed for the samples $Ca_{(1-2x)}Dy_xNa_xBPO_5$ (x = 0, 0.005, 0.01, 0.02, 0.03, 0.04, 0.05), the crystal structure of $CaBPO_5$ is not changed when the doped $Dy^{3+}$ ions enter into the host lattice, as $Dy^{3+}$ and $Na^+$ ions occupy $Ca^{2+}$ normal sites.

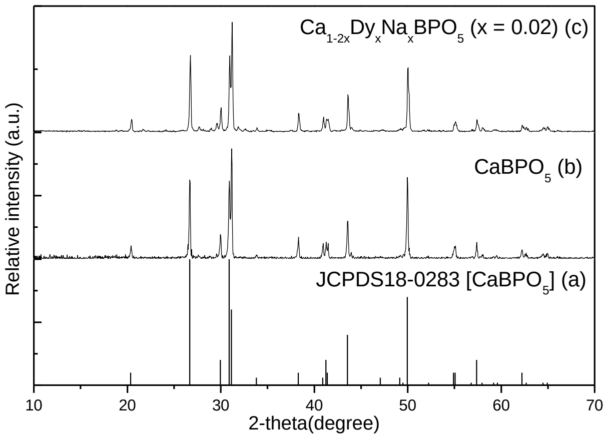


*Fig. 1. XRD patterns of samples $CaBPO_5$, and $Ca_{1-2x}Dy_xNa_xBPO_5$(x = 0.02).*

The UV excitation spectra and the emission spectra under 347 nm excitation for the phosphor $Ca_{1-2x}Dy_xNa_xBPO_5$ (x = 0.02) are shown in Fig. 2. Curve a displays the UV excitation spectrum by monitoring the emission of $Dy^{3+}$ at 479 nm. A series of absorption lines can be observed in the curve, which correspond with the intraconfigurational $4f^9$-$4f^9$ transitions of $Dy^{3+}$ in $CaBPO_5$. The ground state of $Dy^{3+}$ is $^6H_{15/2}$, the transition from this state to different excitation levels are read to be 294 ($^4K_{13/2}$, $^4H_{13/2}$, $^4F_{3/2}$, $^4D_{7/2}$), 322 ($^6P_{3/2}$), 347 ($^4I_{11/2}$, $^4M_{15/2}$, $^6P_{7/2}$), 363 ($^4P_{3/2}$, $^6P_{3/2}$, $^6P_{5/2}$), 384 ($^4M_{21/2}$, $^4I_{13/2}$, $^4F_{7/2}$) nm, respectively, in Fig. 2. The host-related absorption band, $Dy^{3+}$-$O^{2-}$ charge-transfer band and $4f^9$-$4f^85d$ excitation band of $Dy^{3+}$ were not observed in the short wavelength range. This is because they have popularly high energy, and located below 200 nm [15].

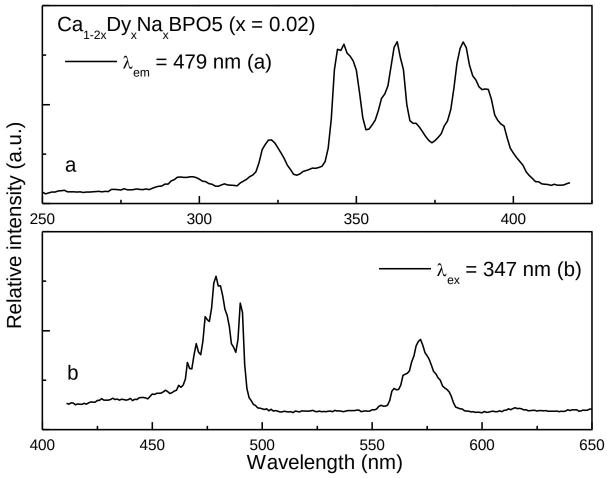


*Fig. 2. UV excitation spectra (a) by monitoring $^4F_{9/2}\rightarrow$ $^6H_{15/2}$ transition of $Dy^{3+}$ and emission spectra under 347 nm excitation of sample $Ca_{1-2x}Dy_xNa_xBPO_5$(x = 0.02).*

The emission spectra upon 347 nm excitation are exhibited in Fig. 2(b). Two $^4F_{9/2}\rightarrow{}^6H_J$ ($J$ = 13/2, 15/2) lines are observed in the curve, in which the blue $^4F_{9/2}\rightarrow{}^6H_{15/2}$ emission at about 479 nm are strong, and whereas the yellow $^4F_{9/2}\rightarrow{}^6H_{13/2}$ emission at about 572 nm are weak. The crystal splitting components of $Dy^{3+}$ emission can be observed, but not totally resolved due to the weak experimental resolution. The $^4F_{9/2}\rightarrow{}^6H_{13/2}$ transition belongs to the hypersensitive transition with $\Delta J$ = 2, which is strongly influenced by the local environment of $Dy^{3+}$ in the host. So the $Dy^{3+}$ site must be highly symmetric because the emission intensity of $^4F_{9/2}\rightarrow{}^6H_{15/2}$ transition is more than that of $^4F_{9/2}\rightarrow{}^6H_{13/2}$ transition. The result indicated that the local symmetry of $Dy^{3+}$ belongs to the inversion symmetry in the host $CaBPO_5$.

The chromaticity coordinate (x, y) of the sample $Ca_{1-2x}Dy_xNa_xBPO_5$(x = 0.02) was calculated in term of the emission under 347 nm excitation and is showed in Fig. 3. The CIE color coordinate of $Ca_{1-2x}Dy_xNa_xBPO_5$(x = 0.02) is (0.287, 0.297) with the relative color temperature of 9357 K, which is located in white light region.

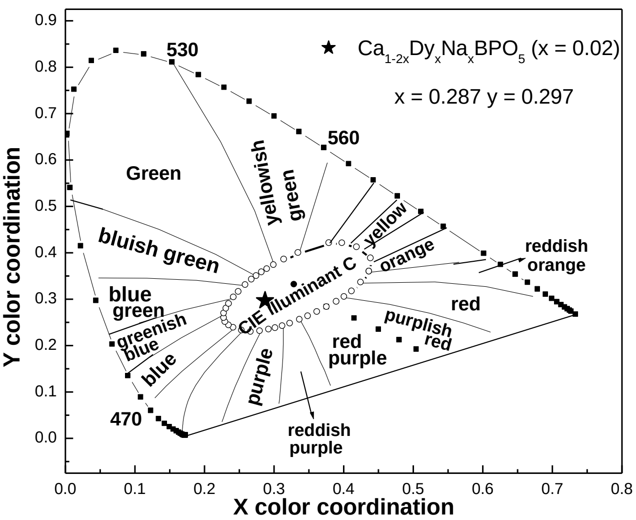


*Fig. 3. The CIE color coordinates of $Ca_{1-2x}Dy_xNa_xBPO_5$(x = 0.02).*

Finally, the luminescence intensity of phosphor materials is known to be dependent on the doping concentration of luminescent ions [16]. Fig. 4 shows the luminescent intensity of the $^4F_{9/2}\rightarrow{}^6H_{13/2}$ transition (479 nm) versus $Dy^{3+}$ concentration in $Ca_{1-2x}Dy_xNa_xBPO_5$ powders under 347 nm excitation. The most efficient luminescence intensities occur for a $Dy^{3+}$ content of x = 0.02. The drop in intensity as the $Dy^{3+}$ content increase is due to the rise in nonradiative decay channels, which are promoted by the interaction with quenching centers during the energy transfer processes among $Dy^{3+}$ ions (concentration quenching effect). Moreover, cross-relaxation occurs easily between two neighbouring rare-earth ions. This is the process whereby excitation energy from an ion decaying from a highly excited state promotes a nearby ion from the ground state to the metastable level. In the case of $Dy^{3+}$ the energy of the $^4F_{9/2}\rightarrow{}^6F_{11/2} + {}^6H_{9/2}$ transition matches the one of the $^6H_{15/2}\rightarrow{}^6F_{11/2} + {}^6H_{9/2}$ transition [17, 18]. With the increase of $Dy^{3+}$ concentration, the distance between $Dy^{3+}$ ions decreases; subsequently, the energy transfer between $Dy^{3+}$ ions becomes more frequent. Therefore, the energy transfer process between the $Dy^{3+}$ ions provides an extra decay channel to quench the luminescence of $Dy^{3+}$ ions.

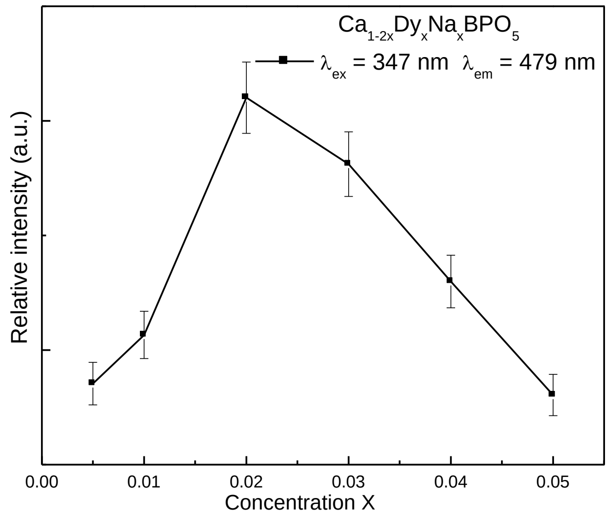


*Fig. 4. The concentration dependence of the luminescence intensity of $Ca_{1-2x}Dy_xNa_xBPO_5$ phosphors.*

The emission intensity (I) per activator concentration (x) can be expressed by the following equation [19, 20]:

$$\frac{I}{x} = \frac{k}{1+\beta(x)^{\theta/3}} \quad (1)$$

where k and β are constants for each interaction for a given host lattice; θ = 6, 8, 10 for dipole-dipole, dipole-quadrupole, quadrupole-quadrupole interactions, respectively. Fig. 5 illustrates the I/x dependence upon x on a logarithmic scale. The dependence of lg(I/x) on lg(x) was found to be relatively linear and the slope (-θ/3) was determined to be -1.96. Thus, the value of θ could be calculated as 5.88, which was close to 6. This indicated that dipole–dipole interaction dominated the concentration quenching mechanism of $Dy^{3+}$ emission.

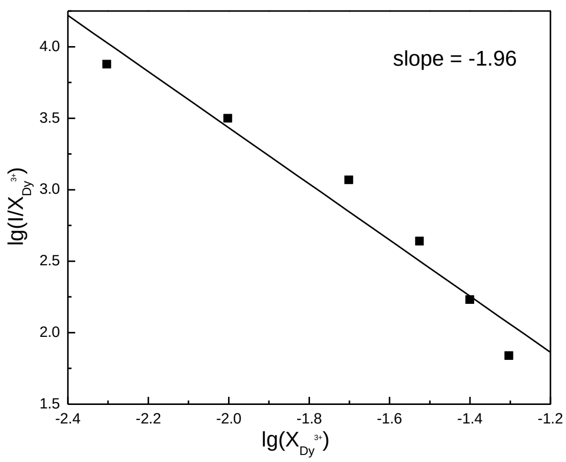


*Fig. 5. The $I/x_{Dy3+}$ dependence of $x_{Dy3+}$ on a logarithmic scale.*

## 4. Conclusions

In summary, $Ca_{1-2x}Dy_xNa_xBPO_5$ samples were prepared by a high-temperature solid-state reaction. The optimum doping concentration is 0.02 (x value) in terms of the relative intensity under 347 nm excitation. The $CaBPO_5:Dy^{3+},Na^+$ phosphor shows two emission peaks at 479 (blue) and 572 nm (yellow) upon the excitation of 347 nm. A white light was generated from $CaBPO_5:0.02Dy^{3+},0.02Na^+$ phosphor with CIE chromaticity coordinates of (x = 0.287, y = 0.297) and relative color temperature of 9357 K. The present study demonstrates $CaBPO_5:Dy^{3+},Na^+$ is potentially a good candidate as an UV-convertible phosphor for white light-emitting diodes (LEDs).

**Acknowledgments**

The work is financially supported by the Science and Technology Research Key Project of Education Department of Henan Province (no. 12A430021) and Scientific Research Foundation for Doctors of Zhengzhou University of Light Industry (no. 2010BSJJ013).

## References

[1] H. A. Höppe, Angew. Chem. Int. Ed. **48**, 3572 (2009).
[2] H. S. Jang, H. Yang, S. W. Kim, J. Y. Han, S. G. Lee, D. Y. Jeon, Adv. Mater. **20**, 2696 (2008).
[3] Y. S. Tang, S. F. Hu, W. C. Ke, C. C. Lin, N. C. Bagkar, R. S. Liu, Appl. Phys. Lett. **93**, 131114 (2008).
[4] R. S. Liu, Y. H. Liu, N. C. Bagkar, S. F. Hu, Appl. Phys. Lett. **91**, 061119 (2007).
[5] J. S. Kim, P. E. Jeon, Y. H. Park, J. C. Choi, H. L. Park, Appl. Phys. Lett. **82**, 3696 (2004).
[6] T. W. Kuo, W. R. Liu, T. M. Chen, Opt. Express **18**(3), 1888 (2010).
[7] T. W. Kuo, W. R. Liu, T. M. Chen, Opt. Express **18**(8), 8187(2010).
[8] Q. Y. Zhang, C. H. Yang, Y. X. Pan, Nanotechnology **18**, 145602 (2007).
[9] J. P. Zhong, H. B. Liang, B. Han, Z. F. Tian, Q. Su, Opt. Express **16**(10), 7508 (2008).
[10] X. M. Liu, R. Pang, Q. Li, J. Lin, J. Solid State Chem. **180**, 1421 (2007).
[11] K. Mini Krishna, G. Anoop, M. K. Jayaraj, J. Electrochem. Soc. **154**(10), 310 (2007).
[12] Q. Su, H. B. Liang, C. Y. Li, H. He, Y. H. Lu, J. Li, Y. Tao, J. Lumin. **122-123**, 927 (2007).
[13] R. Kniep, G. Gozel, B. Eisenmann, C. Rohr, M. Asbrand, M. Kizilyalli, Angew. Chem. Int. Ed. Engl. **33**, 749 (1994).
[14] H. B. Liang, J. S. Shi, Q. Su, S. Y. Zhang, Y. Tao, Mater. Chem. Phys. **92**, 180 (2005).
[15] B. Han, H. B. Liang, H. H. Lin, W. P. Chen, Q. Su, G. T. Yang, G. B. Zhang, J. Opt. Soc. Am. B **25**(12), 2057 (2008).
[16] G. Blasse, B. C. Grabmaier, Luminescent Materials (Springer-Verlag Berlin Heidelberg 1994).
[17] Y. C. Li, Y. H. Chang, Y. F. Lin, Y. S. Chang, Y. J. Lin, J. Alloys Compd. **439**, 367 (2007).
[18] L. Nagli, D. Bunimovich, A. Katzir, O. Gorodetsky, V. Molev, J. Non-Cryst. Solids **217**, 208 (1997).
[19] L. G. Van Uitert, J. Electrochem. Soc. **114**(10), 1048 (1967).
[20] D. L. Dexter, J. Chem. Phys. **21**(5), 836 (1953).

*Corresponding author: hanbing@zzuli.edu.cn